T and NK cell immunity after hematopoietic stem cell transplantation

Lugthart, G.

Chapter 5

$CD56^{dim}CD16^{-}$ NK cell phenotype can be induced by cryopreservation

Published in:
Blood
2015; 125: 1842-1843

Gertjan Lugthart
Monique M. van Ostaijen-ten Dam
Maarten J.D. van Tol
Arjan C. Lankester *and*
Marco W. Schilham

Abstract

Early after hematopoietic stem cell transplantation, NK cells are temporary susceptible to cryopreservation-induced phenotypic changes. This emphasizes the importance to validate flowcytometric results with fresh PBMC samples to become aware of potential situation-specific cryopreservation-induced phenotypic changes.

To the editor:

Natural Killer (NK) cells can contribute to the control of different viruses.[218;219] Recently, Azzi and colleagues described the role of early-differentiated NK cells in Epstein-Barr virus driven infectious mononucleosis (IM).[121] Besides the conventional $CD56^{bright}CD16^{+/-}$ and $CD56^{dim}CD16^{+}$ NK cell populations, a phenotypically distinct $CD56^{dim}CD16^{-}$ NK cell population was transiently observed during acute IM.

We have also observed this $CD56^{dim}CD16^{-}$ NK cell phenotype in cryopreserved PBMC from hematopoietic stem cell transplantation (HSCT) recipients, especially early after transplantation. However, only the conventional $CD56^{bright}CD16^{+/-}$ and $CD56^{dim}CD16^{+}$ NK cells were detected in freshly analyzed PBMC, indicating that the $CD56^{dim}CD16^{-}$ phenotype is induced by cryopreservation (Figure 5.1A).

Blood samples were obtained from 9 pediatric HSCT recipients and 4 healthy donors after written informed consent and approval by the institutional review board (protocol P02.099). PBMC were isolated using ficoll-isopaque separation within 6h after blood withdrawal and analyzed by flowcytometry. The remainder of cells was cryopreserved in liquid nitrogen, thawed and reanalyzed. NK cells were defined as $CD19^{-}CD3^{-}CD7^{+}CD56^{+}/16^{+/-}$ cells within the live ($DAPI^{-}$) $CD45^{+}$ $CD14^{-}CD33^{-}CD235a^{-}$ lymphocyte gate.[230]

In fresh PBMC, $CD56^{dim}CD16^{-}$ cells constituted <3% of NK cells, mainly caused by overspill from $CD56^{bright}CD16^{+/-}$ or $CD56^{dim}CD16^{+}$ NK cells.[105;231] In contrast, $CD56^{dim}CD16^{-}$ cells represented a larger and distinct population in cryopreserved PBMC (Figure 5.1 A-B). These cells accounted for 17-36% of cryopreserved NK cells at 3 weeks after HSCT (fresh vs. cryopreserved: $p<0.001$, paired t-test), rapidly decreasing in the weeks thereafter (Figure 5.1 C-D). This $CD56^{dim}CD16^{-}$ NK cell population was identified with various monoclonal antibodies (CD56-clones N901/HCD56; CD16-clones 3G8/B73.1). Interestingly, the cryopreservation-induced $CD56^{dim}CD16^{-}$ population was also enlarged when healthy donor blood was stored for 24h at room temperature before PBMC were isolated (Figure 5.1E), suggesting a relationship with the vitality of PBMC prior to cryopreservation.[232;233]

We hypothesized that the cryopreservation induced $CD56^{dim}CD16^{-}$ NK cells originated from either $CD56^{bright}CD16^{+/-}$ or $CD56^{dim}CD16^{+}$ NK cells as a consequence of reduced CD56 or CD16 expression, respectively. At three weeks after HSCT, predominantly the largest $CD56^{bright}CD16^{+/-}$ NK cell population was decreased after cryopreservation (mean 67 to 46% of NK cells, $p=0.002$), coinciding with the appearance of the $CD56^{dim}CD16^{-}$ phenotype. One week later, both a reduction of $CD56^{bright}CD16^{+/-}$ (45 to 36%, $p=0.01$) and $CD56^{dim}CD16^{+}$ (54 to 41%, $p=0.01$) NK cells was observed. At one year after HSCT and in healthy donors, $CD56^{dim}CD16^{+}$ NK cells formed the majority of NK cells and mainly this phenotype was reduced after cryopreservation (Figure 5.1 C-E). Thus, depending on time after HSCT, both $CD56^{bright}CD16^{+/-}$ and $CD56^{dim}CD16^{+}$ NK cells could contribute to the $CD56^{bright}CD16^{+/-}$ phenotype.

A skewing towards the early-differentiated $NKG2A^{+}KIR^{-}$ NK cell phenotype is observed early after HSCT as well as during acute IM[121;126], raising the possibility that these cells might be particularly sensitive to cryopreservation. However, the presence of $NKG2A^{+}KIR^{-}$ NK cells and occurrence of $CD56^{dim}CD16^{-}$ NK cells showed different kinetics (Figure 5.1 F-G). In multivariate

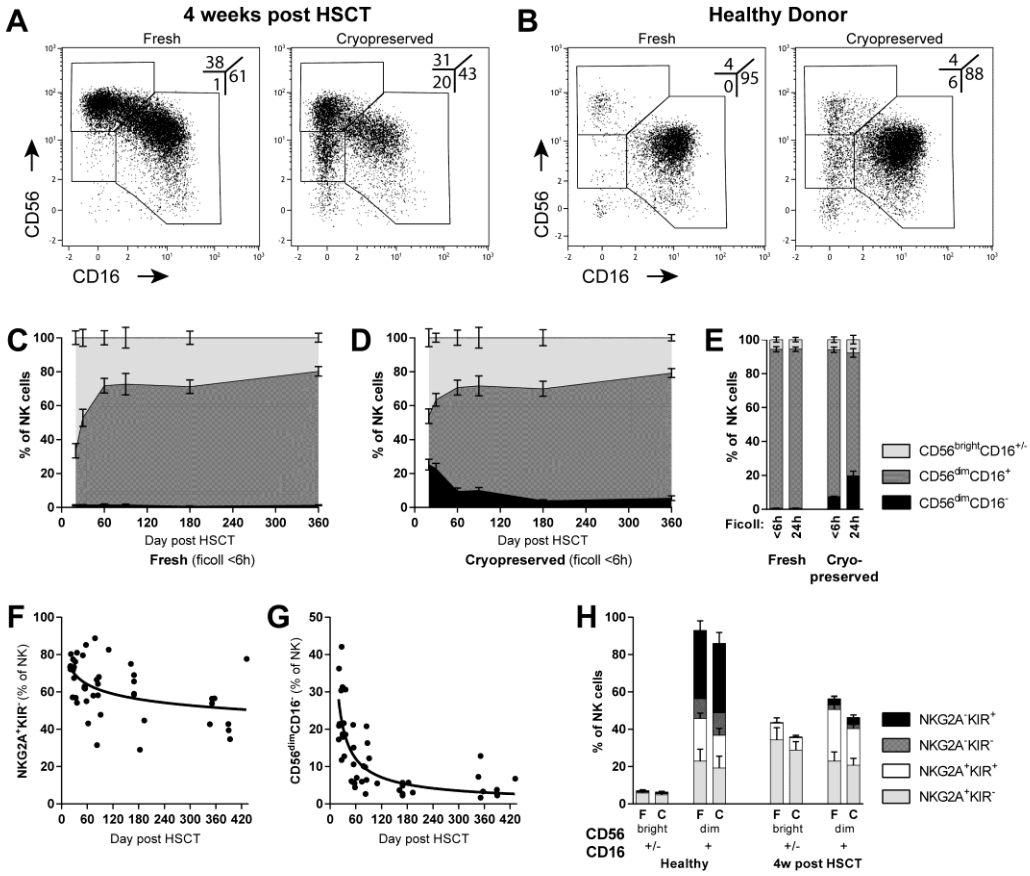

Figure 5.1. CD56^{dim}CD16^{-} NK cell phenotype can be induced by cryopreservation.
(A-B) Representative FACS plots of fresh and cryopreserved NK cells from hematopoietic stem cell transplantation (HSCT) recipients at 4 weeks after transplantation (A) and healthy donors (B). **(C-D)** Longitudinal NK cell reconstitution in 9 HSCT recipients based on the paired evaluation of fresh (C) and cryopreserved (D) PBMC. Shown is the contribution (mean +/- SEM) of CD56^{bright}CD16$^{+/-}$ (light gray), CD56^{dim}CD16^{+} (dark gray) and CD56^{dim}CD16^{-} cells (black) to the NK cell compartment. **(E)** Evaluation of fresh (left) and cryopreserved (right) NK cells after direct (<6h) or delayed (24h) separation of PBMC from EDTA blood. Shown is the mean +- SEM of 4 healthy donors.
(F-G) Contribution of early-differentiated NKG2A^{+}KIR^{-} NK cells (F) and cryopreservation-induced CD56^{dim}CD16^{-} NK cells (G) to the total NK cell population, expressed as a function of time after HSCT. (H) Differentiation of NK cells based on the expression of NKG2A and KIRs on NK cells in fresh (F) and cryopreserved (C) PBMC. Shown is the percentage of NKG2A^{+}KIR^{-} (light gray), NKG2A^{+}KIR^{+} (white), NKG2A^{-}KIR^{+} (dark gray) and NKG2A^{-}KIR^{+} (black) NK cells divided over the CD56^{bright}CD16$^{+/-}$ and CD56^{dim}CD16^{+} NK cell phenotypes. Bars represent mean +/- SEM of 4 healthy donors or 2 HSCT recipients at 4 weeks after transplantation.

analysis, the percentage of CD56^{dim}CD16^{-} cells was only correlated with time after HSCT and not to the percentage of NKG2A^{+}KIR^{-} cells (*p<0.0001 vs. p=0.35*, linear regression on log-transformed data). Importantly, no significant differences were observed between the NKG2A/KIR phenotype of CD56^{dim}CD16^{+} and CD56^{bright}CD16$^{+/-}$ NK cells when analyzed before and after cryopreservation (Figure 5.1H).

Altogether, NK cells are temporarily more sensitive to cryopreservation-induced phenotype changes in the first weeks after HSCT. This might relate to the $CD56^{dim}CD16^{-}$ NK cell phenotype which was transiently observed during the acute phase of IM.[121] Both during acute IM and early after HSCT, $CD56^{dim}CD16^{-}$ NK cells are observed under inflammatory conditions. This raises the possibility that cryopreservation-induced phenotypic changes are related to activation-associated cellular mechanisms.

Clinical situations like the absence of T cells after HSCT or viral infections provide unique opportunities to study human NK cell biology. It should be taken into account that under such circumstances, NK cells may be transiently susceptible to cryopreservation-induced phenotype changes. Since the $CD56^{dim}CD16^{-}$ NK cells can originate from both conventional NK cell populations, we recommend to assess the cryopreservation-induced $CD56^{dim}CD16^{-}$ NK cells separately to avoid phenotype-skewing of the conventional populations. Our data emphasize the importance to validate flowcytometric results with fresh PBMC samples to become aware of potential cryopreservation-induced phenotypic changes.

Funding and Disclosures

This work was supported by the Dutch Cancer Society (grant UL-2011-5133). GL was supported by a Leiden University Medical Center MD/PhD fellowship.

Gating strategy

FACS-data were acquired on a Becton Dickinson (*BD*) LSRII flow cytometer and analyzed using Beckman Coulter (*BC*) Kaluza software.

Gating strategy (Figure 5.1 A-E, G): Forward scatter vs. $DAPI^{-}$(*Sigma-Aldrich*): live→ $CD45^{+}$(FITC, *clone 2D1, BD*) vs. $CD14^{-}$(PE, *MOP9, BD*) & $CD33^{-}$(PE, *P67.6, BD*) & $CD235a^{-}$(PE, *KC16, BC*) →$CD19^{-}$(APC, *J4.119, BC*) → $CD3^{-}$(BrilliantViolet421, *UCHT1, BD*) vs. $CD7^{+}$(Alexa700, *M-T701, BD*) →CD56(PE-Texas Red, *N901, BC*) vs. CD16(BV711, *3G8, BD*).

Gating strategy (Figure 5.1 F & H): Forward scatter vs $DAPI^{-}$(*Sigma-Aldrich*): live→ $CD14^{-}$(APC, *MOP9, BD*) & $CD19^{-}$ (APC, *J4.119, BC*) → $CD3^{-}$(BrilliantViolet421, *UCHT1, BD*) vs. $CD7^{+}$(Alexa700, *M-T701, BD*) →CD56(PE-Texas Red, *N901, BC*) vs. CD16(BV711, *3G8, BD*) →NKG2A (PE-Cy7, *Z199, BC*) vs. KIR (PE, combination of CD158e + a/h + i + b/j (*DX9, BD + EB6, BC + FES172, BC + GL183, BC*)).